MIXED BOUNDARY VALUE PROBLEMS IN SOIL MECHANICS[1]

By
R. T. SHIELD[2]
Brown University

Summary. The stress-strain law for an ideal soil formulated in a recent paper [1][3] is applied here to obtain the velocity equations referred to the stress characteristic lines in plane strain problems. Simple velocity fields associated with families of straight characteristic lines are then examined, together with discontinuities in the velocity field. The results are applied to obtain the incipient velocity field for the indentation of a semi-infinite mass of material by a flat punch or footing, and to solve the problem of indentation by a lubricated wedge.

1. Introduction. In deriving the solutions of two-dimensional problems in soil mechanics, it is usual to assume that the soil is a plastic material in which slip or yielding occurs when the stresses satisfy the Coulomb formula [2]

$$f = \frac{\sigma_x + \sigma_y}{2} \sin \varphi + \sqrt{\frac{1}{4}(\sigma_x - \sigma_y)^2 + \tau_{xy}^2} - c \cos \varphi = 0, \tag{1}$$

where c is the cohesion and φ is the angle of internal friction of the soil. The stresses also satisfy the equilibrium equations

$$\left.\begin{aligned} \frac{\partial \sigma_x}{\partial x} + \frac{\partial \tau_{xy}}{\partial y} &= 0, \\ \frac{\partial \tau_{xy}}{\partial x} + \frac{\partial \sigma_y}{\partial y} &= 0, \end{aligned}\right\} \tag{2}$$

in which the weight of the soil is neglected. The equations (1), (2) are hyperbolic and the two characteristic directions are inclined at an angle $\pi/4 + \varphi/2$ to the direction of the algebraically greater principal stress. In Fig. 1, the lines 1, 2 are the directions of the

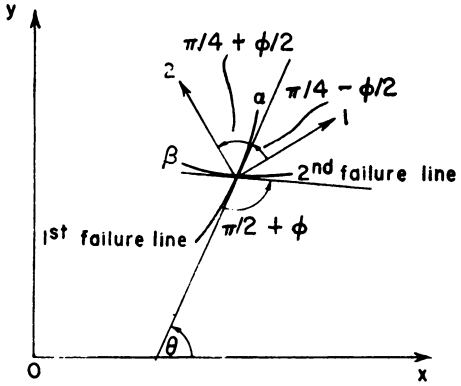

FIG. 1. Failure Lines

Received March 17, 1952.

[1]The results presented in this paper were obtained in the course of research sponsored by the Office of Naval Research under Contract N7onr-358 (Task Order 1) with Brown University.

[2]Research Associate, Graduate Division of Applied Mathematics, Brown University.

[3]Numbers in square brackets refer to the bibliography at the end of the paper.

principal stresses σ_1 , σ_2 ($\sigma_1 < \sigma_2$) at a point and the lines α, β are the characteristic lines passing through the point. We shall call the characteristic line which lies between the 1 and 2 directions the first failure line and denote by θ the angle of inclination of this line to the x-axis.

If we now put

$$p = \frac{(\sigma_2 - \sigma_1)}{2m \sin \varphi} \geq 0, \tag{3}$$

where m is a positive constant which has the dimensions of stress, then, using (1), it can be shown [3] that

$$\left.\begin{aligned} \sigma_x &= -mp[1 + \sin \varphi \sin (2\theta + \varphi)] + c \cot \varphi, \\ \sigma_y &= -mp[1 - \sin \varphi \sin (2\theta + \varphi)] + c \cot \varphi, \\ \tau_{xy} &= mp \sin \varphi \cos (2\theta + \varphi). \end{aligned}\right\} \tag{4}$$

The equations of equilibrium (2) can be replaced by the equations

$$\left.\begin{aligned} \tfrac{1}{2} \cot \varphi \log p + \theta &= \text{const.} \qquad \text{along a first failure line,} \\ \tfrac{1}{2} \cot \varphi \log p - \theta &= \text{const.} \qquad \text{along a second failure line,} \end{aligned}\right\} \tag{5}$$

which were first obtained by Kötter [4].

The three stress components, σ_x , σ_y and τ_{xy} , are determined from the equilibrium equations (2) and the yield condition (1); alternatively, they can be determined by integrating equations (5) along the failure lines. The usual treatment of plane-strain problems assumes that the problems are statically determinate. In general, however, the stress boundary conditions are not sufficient to make the problem statically determinate and a stress-strain law is necessary in order to allow a more complete investigation of the problem. In the following we shall use a stress-strain law which is derived by assuming that the soil is a perfectly plastic body. It should be remarked that this assumption neglects many practical effects (such as the presence of water in the soil). The predictions of the theory must be compared with the actual behavior of soil in order to obtain an indication of the value of the assumption.

2. The velocity field. Drucker and Prager considered a proper generalization of the Coulomb hypothesis (1) and they showed that if the soil is assumed to be a plastic material then, according to the concept of plastic potential [5], the stress-strain law for plane strain corresponding to the yield function (1) is

$$\left.\begin{aligned} \epsilon_x &= \lambda \frac{\partial f}{\partial \sigma_x} = \frac{\lambda}{2}\left\{\sin \varphi + \frac{(\sigma_x - \sigma_y)/2}{[\tfrac{1}{4}(\sigma_x - \sigma_y)^2 + \tau_{xy}^2]^{1/2}}\right\}, \\ \epsilon_y &= \lambda \frac{\partial f}{\partial \sigma_y} = \frac{\lambda}{2}\left\{\sin \varphi - \frac{(\sigma_x - \sigma_y)/2}{[\tfrac{1}{4}(\sigma_x - \sigma_y)^2 + \tau_{xy}^2]^{1/2}}\right\}, \\ \gamma_{xy} &= \lambda \frac{\partial f}{\partial \tau_{xy}} = \lambda \frac{\tau_{xy}}{[\tfrac{1}{4}(\sigma_x - \sigma_y)^2 + \tau_{xy}^2]^{1/2}}, \end{aligned}\right\} \tag{6}$$

where ϵ_x , ϵ_y , γ_{xy} are the plastic strain rates and λ is a positive factor of proportionality which may assume different values for different particles. Since we assume that there is

no deformation of the soil until plastic yielding occurs, the plastic strain rate is equal to the total strain rate, and we have

$$\epsilon_x = \frac{\partial u}{\partial x}, \qquad \epsilon_y = \frac{\partial v}{\partial y}, \qquad \gamma_{xy} = \frac{\partial u}{\partial y} + \frac{\partial v}{\partial x},$$

where u, v are the components of velocity along the x, y-axes. Using equations (4), equations (6) can be written

$$\left.\begin{aligned} \epsilon_x &= \frac{\lambda}{2}\{\sin\varphi - \sin(2\theta + \varphi)\}, \\ \epsilon_y &= \frac{\lambda}{2}\{\sin\varphi + \sin(2\theta + \varphi)\}, \\ \gamma_{xy} &= \lambda\cos(2\theta + \varphi). \end{aligned}\right\} \tag{7}$$

From the stress-strain relations (6) or (7), the rate of dilation is found to be

$$\epsilon_x + \epsilon_y = \lambda \sin\varphi \geq 0, \tag{8}$$

so that an important feature of the relations is that plastic deformation must be accompanied by an increase in volume if $\varphi \neq 0$.

If we put $\theta = 0$ and $\theta = -(\pi/2 + \varphi)$ in turn in the first equation of equations (7) we find that

$$\left(\frac{\partial u}{\partial x}\right)_{\theta=0} = \left(\frac{\partial u}{\partial x}\right)_{\theta=-(\pi/2+\varphi)} = 0. \tag{9}$$

These equations express the fact that the rate of extension along the failure lines is zero.

The components u, v of the velocity vector are to be determined from equations (7) when the pattern of the failure lines is known for a given plastic stress field. It can easily be shown that the characteristics of the velocities coincide with the characteristics of the stresses and it is more convenient to refer the velocity equations to the characteristic lines. We denote by v_1 and v_2 the *orthogonal projections* of the velocity vector at a point on the directions of the first and second failure lines passing through the point (see Fig. 2). The signs of these velocity projections are chosen so that a counterclock-

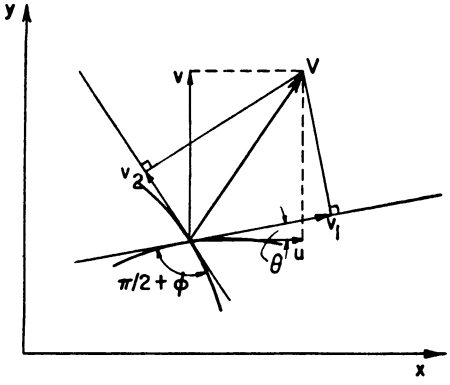

FIG. 2. Velocity Projections

wise rotation of the positive direction along the first failure line through an angle of $\pi/2 + \varphi$ transforms it into the positive direction along the second failure line. The velocity projections v_1 , v_2 are related to the cartesian components u, v of the velocity by the equations

$$\left.\begin{aligned} v_1 &= u\cos\theta + v\sin\theta, & v_2 &= -u\sin(\theta+\varphi) + v\cos(\theta+\varphi), \\ u &= \frac{v_1\cos(\theta+\varphi) - v_2\sin\theta}{\cos\varphi}, & v &= \frac{v_1\sin(\theta+\varphi) + v_2\cos\theta}{\cos\varphi}. \end{aligned}\right\} \tag{10}$$

The substitution of these equations into equations (9), which state that the rate of extension along the failure lines is zero, gives the equations of the velocity field referred to the characteristic lines,

$$\left.\begin{aligned} dv_1 - (v_1\tan\varphi + v_2\sec\varphi)\,d\theta &= 0 \qquad \text{along a first failure line,} \\ dv_2 + (v_1\sec\varphi + v_2\tan\varphi)\,d\theta &= 0 \qquad \text{along a second failure line.} \end{aligned}\right\} \tag{11}$$

These equations can also be obtained as follows. In Fig. 3, A and B represent two neigh-

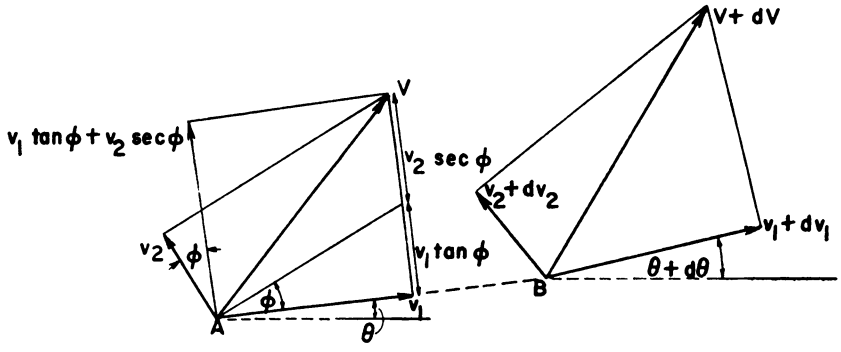

FIG. 3. Inextensibility of failure lines.

boring points on a first failure line separated by an infinitesimal distance ds_1 . The end points of the element AB move with the velocities indicated in the figure. The extension of the element may be considered to be caused by the following two circumstances: (i) the velocity along the element at A is smaller than the corresponding velocity at B by an amount dv_1 , and (ii) the normal component of the velocity at A and the normal component of the velocity at B are inclined at an angle $d\theta$. The corresponding rates of extension are dv_1/ds_1 and $-(v_1\tan\varphi + v_2\sec\varphi)\,d\theta/ds_1$, since the normal component of velocity at A is $v_1\tan\varphi + v_2\sec\varphi$. The condition that the total rate of extension along a first failure line must be zero is therefore

$$dv_1 - (v_1\tan\varphi + v_2\sec\varphi)\,d\theta = 0$$

along a first failure line. This is the first of equations (11) and the second equation can be obtained in a similar manner.

Equations (11), together with the velocity boundary conditions and the condition that the dilatation must be positive, suffice to determine the velocity field when the failure lines are known.

3. Families of straight failure lines. The simplest pattern of failure lines consists of two families of straight lines intersecting at an angle $\pi/2 + \varphi$. As can be seen from equations (5), this pattern corresponds to a region of constant stress and it is usually called an active Rankine zone or a passive Rankine zone in the literature of soil me-

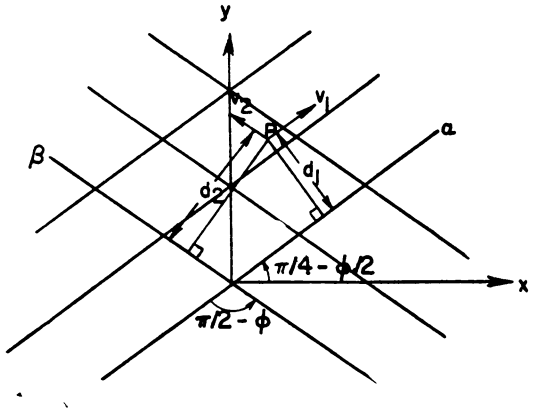

FIG. 4. Region of Constant Stress.

chanics. In Fig. 4, the x and y axes are taken along the directions of the minimum and maximum principal stresses respectively. Since θ is constant along the failure lines, equations (11) show that v_1 is constant along a first failure line and v_2 is constant along a second failure line. If we denote by d_1 and d_2 the distances of a current point from one of the first failure lines and one of the second failure lines, say the failure lines which pass through the origin, then we can write

$$v_1 = f(d_1), \qquad v_2 = g(d_2),$$

where

$$d_1 = -x \sin\left(\frac{\pi}{4} - \frac{\varphi}{2}\right) + y \cos\left(\frac{\pi}{4} - \frac{\varphi}{2}\right),$$

$$d_2 = x \sin\left(\frac{\pi}{4} - \frac{\varphi}{2}\right) + y \cos\left(\frac{\pi}{4} - \frac{\varphi}{2}\right),$$

and where the functions f and g are such that the dilatation is positive everywhere in the region. The cartesian components of the velocity vector are found from (10) to be

$$u = \left\{f(d_1) \cos\left(\frac{\pi}{4} + \frac{\varphi}{2}\right) - g(d_2) \sin\left(\frac{\pi}{4} - \frac{\varphi}{2}\right)\right\} \Big/ \cos\varphi,$$

$$v = \left\{f(d_1) \sin\left(\frac{\pi}{4} + \frac{\varphi}{2}\right) + g(d_2) \cos\left(\frac{\pi}{4} - \frac{\varphi}{2}\right)\right\} \Big/ \cos\varphi.$$

When one of the families of failure lines consists of concurrent straight lines, the other family is a system of logarithmic spirals which have the point of intersection as centre. This stress distribution is usually called a zone of radial shear. In Fig. 5 we have

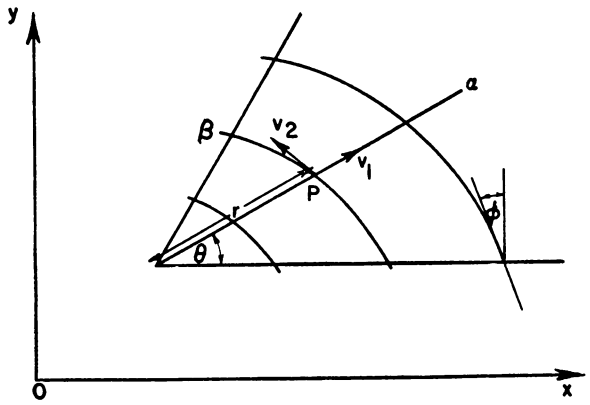

FIG. 5. Zone of Radial Shear.

taken the first failure lines to be the family of straight lines and we denote by r the distance from the centre of the spirals. Since θ is constant along the first failure lines, v_1 is constant along these lines and we have

$$v_1 = f(\theta).$$

Substituting for v_1 in the second of equations (11) we obtain

$$v_2 e^{\theta \tan\varphi} = -\sec\varphi \int_{\theta_0}^{\theta} f(\theta) e^{\theta \tan\varphi}\, d\theta + A$$

along a second failure line. In this equation A is a constant of integration which is constant along each second failure line but which may take different values on different second failure lines. Since the spirals are given by the equation

$$re^{\theta \tan\varphi} = \text{constant},$$

the function A can be written in the form

$$A = g(re^{\theta \tan\varphi}).$$

The functions f and g must be such that the dilatation is positive everywhere in the region. When $f(\theta)$ is zero, i.e., when v_1 is zero, we obtain

$$v_2 = Ae^{-\theta \tan\varphi},$$

so that v_2 varies exponentially along each second failure line.

If the second failure lines had been taken to be the family of concurrent straight lines then we would have obtained

$$v_2 = f(\theta), \qquad v_1 e^{-\theta \tan\varphi} = \sec\varphi \int_{\theta_0}^{\theta} f(\theta) e^{-\theta \tan\varphi}\, d\theta + A,$$

where A is constant along each first failure line. As before, $f(\theta)$ and A must be such that the dilatation is everywhere positive.

4. Discontinuities in the velocity field. It can be shown, as in the theory for a perfectly plastic material, that a line separating a region of plastic flow from a region which remains at rest must be a failure line. This follows from equations (11) because, if the line were not a failure line, a region at rest on one side of the line would imply a certain region at rest on the other side of the line. This still applies if the velocity field is discontinuous across the line separating the two regions. A line of discontinuity in the velocity field must be regarded as a thin layer producing a continuous transition from one velocity field to another. Since a discontinuity in the tangential velocity must be accompanied by a separation or discontinuity in the normal velocity, the transitional layer must have appreciable thickness for a soil while there is no need for such a layer in a Prandtl-Reuss material (for which $\varphi = 0$).

Let P be a point on the median line of such a transitional layer and take the x, y axes along the tangential and normal directions at P. Since, at P, $\partial u/\partial x$ and $\partial v/\partial x$ must be negligible compared with $\partial u/\partial y$, the strain rate ϵ_x must be very small compared with the strain rate γ_{xy} . The stress-strain relations (7) show that this can only be so if we have $\theta = 0$ or π, or $\theta = \pi/2 - \varphi$ or $3\pi/2 - \varphi$, that is, if the line of discontinuity is a first or second failure line respectively. Also from (7), for these values of θ, we have

$$\left.\begin{aligned} \epsilon_y &= \frac{\partial v}{\partial y} = \lambda \sin \varphi, \\ \gamma_{xy} &\doteqdot \frac{\partial u}{\partial y} = \pm\lambda \cos \varphi, \end{aligned}\right\} \tag{12}$$

the positive or negative sign being taken according as the line of discontinuity is a first or second failure line. Equations (12) show that the change in velocity across the line is inclined at angle φ to the line of discontinuity. Further, if we denote by u_1 and u_2 the values of the velocity component u on the sides of the line of smaller and larger values of y, then equations (12) show that $u_2 > u_1$ or $u_1 > u_2$ according as the line of discontinuity is a first or second failure line respectively.

The straight line and the logarithmic spiral of angle φ are the only lines of discontinuity which permit rigid motions, translation and rotation respectively, of the regions separated by the line. These two types of "sliding" discontinuity have been used by Drucker and Prager to obtain upper bounds for the critical height of a vertical bank of soil.

5. Indentation by flat punch. In this section the theory developed above is applied to the indentation of a semi-infinite mass of soil by a flat rigid punch or footing (under conditions of plane strain). A possible plastic stress distribution was determined by Prandtl [6] and we shall consider this stress distribution together with an alternative solution. The two stress distributions, which give the same value for the bearing capacity of the soil, are illustrated in Figs. 6 and 7. They correspond to the two solutions proposed by Prandtl and by Hill [7] for the same problem in a perfectly plastic material (for which $\varphi = 0$). It seems probable that Prandtl's solution is more nearly correct when the punch is sufficiently rough, while the other solution will apply when the surface of the punch is smooth.

Referring to Figs. 6 and 7, plastic regions begin to form at A and B as soon as the load is applied to the punch, but no indentation is possible until the plastic region extends all the way from A to B. We consider only the incipient plastic flow so that the boundary conditions are satisfied at the underformed surface. The problem of determining the stresses and velocities after the punch has penetrated a finite distance is of greater difficulty and would require a study of the successive phases of the plastic flow.

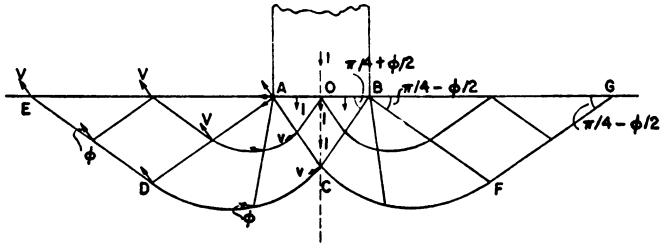

FIG. 6. Prandtl Solution.

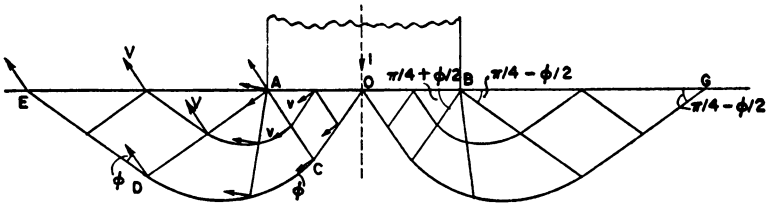

FIG. 7. Alternative Solution

Consider first the solution represented by Fig. 7, and since it is symmetrical about the axis of the punch, we need discuss only the left-hand plastic region. The regions AOC, ADE are regions of constant stress (active and passive Rankine zones respectively), while the region ACD is a zone of radial shear. We take the downward velocity of the punch as the unit of velocity so that along AB the downward component of the velocity of the material must be unity. The material below the second failure line $OCDE$ remains at rest so that $OCDE$ is a line of discontinuity. Thus the velocity along this line is everywhere inclined at an angle φ to the line, i.e., along this line $v_1 = 0$. It follows that $v_1 = 0$ throughout the plastic region since v_1 must be constant along each first failure line.

In the region AOC, v_2 is also constant and the region moves as a rigid body in the direction perpendicular to AC. If v is the velocity of the region then the boundary condition along AO gives

$$v = \sec\left(\frac{\pi}{4} + \frac{\varphi}{2}\right),$$

and we also have

$$v_2 = v \cos \varphi = \cos \varphi \sec \left(\frac{\pi}{4} + \frac{\varphi}{2}\right)$$

in this region. In the zone of radial shear ACD, we have

$$v_2 = Ae^{-\theta \tan \varphi},$$

where A is constant along each second failure line. Since v_2 is constant along AC, we see that v_2 is constant along each first failure line of ACD and also

$$v_2 = \cos \varphi \sec \left(\frac{\pi}{4} + \frac{\varphi}{2}\right) e^{(\tan \varphi)\pi/2}$$

along AD. Finally, the region ADE moves as a rigid body with velocity $V = \sec (\pi/4 + \varphi/2)e^{(\tan \varphi)\pi/2}$ in the direction perpendicular to AD. The velocity field is represented by the small arrows in Fig. 7.

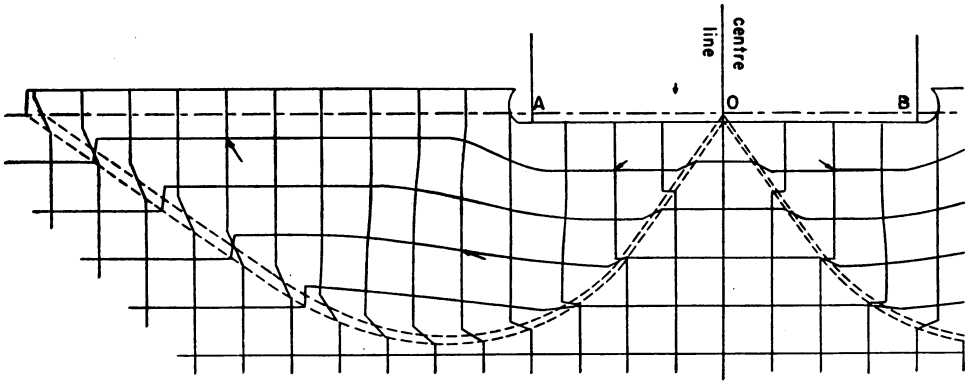

FIG. 8 Resulting deformation of square grid if incipient velocity field was maintained for a short time, according to alternative solution

Figure 8 shows the distortion of a square grid which would result if the initial velocity field was maintained for a short period of time (where φ is taken to be 20°). In obtaining this diagram a thin transition layer was assumed to exist between the line $OCDE$ of Fig. 7 and the material which remains at rest. The initial position of the layer is indicated by broken lines in the figure.

The initial velocity field for the Prandtl solution, Fig. 6, can be obtained in an analogous manner. In this case the region ABC moves downward as a rigid body and the lines AC, BC in addition to the lines CDE, CFG, are lines of discontinuity. As before, we take the downward velocity of the punch as the unit of velocity. Referring to the left-hand side of Fig. 6, the material below the second failure line CDE remains at rest so that the velocity along this line must be inclined at an angle φ to the line. Hence $v_1 = 0$ along this line and since the first failure lines are straight it follows that $v_1 = 0$ in the region $ACDEA$. The velocity of the material just to the left of the discontinuity line AC is perpendicular to AC and its magnitude must be such that the change in velocity across AC is inclined at an angle φ to AC. By drawing the velocity diagram

shown in Fig. 9, we see that the velocity must have the magnitude

$$v = \frac{1}{2}\sec\left(\frac{\pi}{4} + \frac{\varphi}{2}\right).$$

In the zone of radial shear ACD the velocity increases exponentially to the value

$$V = \frac{1}{2}\sec\left(\frac{\pi}{4} + \frac{\varphi}{2}\right)e^{(\tan\varphi)\,\pi/2}$$

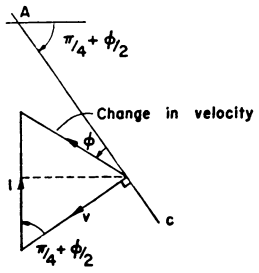

FIG. 9 Velocity diagram for discontinuity line AC in Fig. 6.

on the line AD. The region ADE moves as a rigid body in the direction perpendicular to AD with this velocity V.

The small arrows in Fig. 6 represent the velocity field. The distortion of a square grid which would result if the material moved with this initial velocity field for a short period of time is shown in Fig. 10 (where φ is taken to be 20°). Thin transition layers were assumed to exist between the lines AC, BC and the material in ABC which moves downward with the punch, and a thin transition layer was taken between the line $EDCFG$ and the material at rest. These layers are indicated by the broken lines in Fig. 10.

We notice that the velocity V of the material along AE in the Prandtl solution is

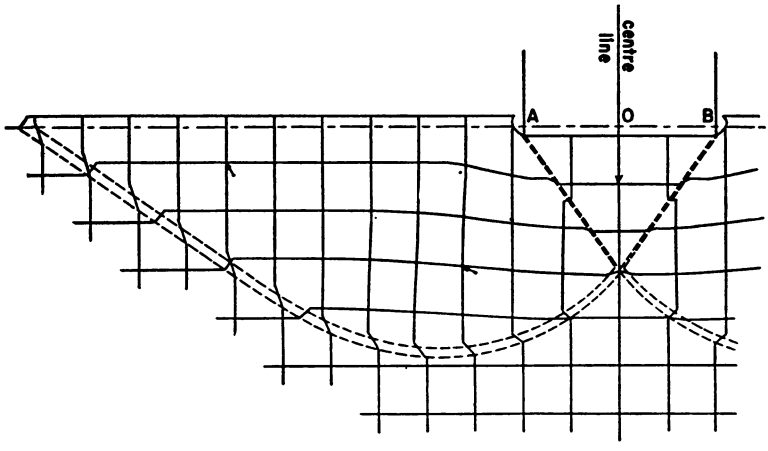

FIG. 10 Resulting deformation of square grid if incipient velocity field was maintained for a short time according to Prandtl solution

exactly half the value of the corresponding velocity in the alternative solution and the velocities are inclined at the same angle, $\pi/4 + \varphi/2$, to the surface AE. For a given width AB of the punch, however, the length of AE in Fig. 6 is twice the length of AE in Fig. 7. It follows that the volume of soil raised above the undisturbed surface after the punch has penetrated a small distance is the same in both solutions.

6. Wedge indentation. We now consider the problem of the indentation of a semi-infinite mass of soil by a smooth, rigid wedge under conditions of plane strain. The solution of the same problem in a perfectly plastic material was obtained by Hill, Lee and Tupper [8], and the solution for the material that we are considering follows this solution closely. Since the configuration is geometrically similar at each stage of the penetration, it is possible to obtain the complete history of the motion without following the deformation step by step.

As the wedge is pressed into the soil, the displaced soil will form a raised lip at each side of the wedge, and the shape of the lips must be determined as part of the solution to the problem. We shall assume that the surfaces of the lips are straight and show that a solution exists which satisfies this assumption. The pattern of failure lines is indicated

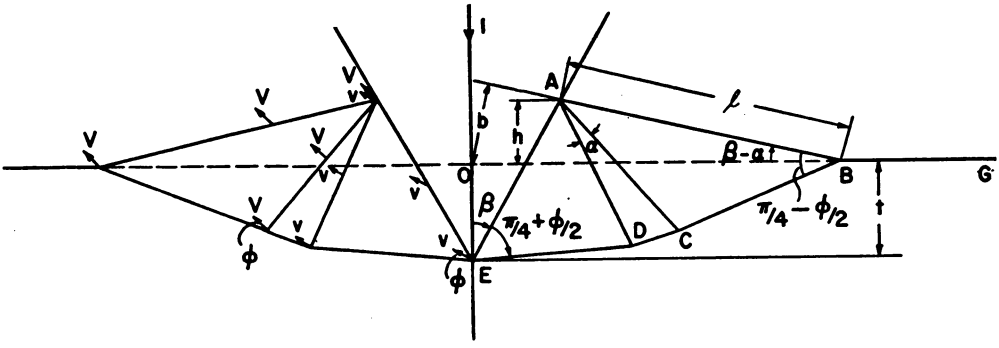

FIG. 11 Indentation by lubricated wedge

in Fig. 11. AE is the right flank of the wedge, which is of angle 2β, BG is the as yet undeformed surface of the soil and AB is the lip. The regions AED, ABC are regions of constant stress while ADC is a zone of radial shear of angle α. We denote by l the length AB of the lip, by b the distance of O from AB, and by h the elevation of A above OB. The depth of penetration of the wedge is denoted by t and if the downward velocity of the wedge is taken as the unit of velocity, we may take t to be the time variable.

The lip AB makes an angle $\beta - \alpha$ with the undisturbed level OB and it is easily shown that we have the following expressions for l, b, h in terms of t, α, β:

$$\left.\begin{aligned} l &= t \Big/ \left\{ e^{-\alpha \tan\varphi} \tan\left(\frac{\pi}{4} - \frac{\varphi}{2}\right) \cos\beta - \sin(\beta - \alpha) \right\}, \\ h &= t \sin(\beta - \alpha) \Big/ \left\{ e^{-\alpha \tan\varphi} \tan\left(\frac{\pi}{4} - \frac{\varphi}{2}\right) \cos\beta - \sin(\beta - \alpha) \right\}, \\ b &= \frac{t \sin(\beta - \alpha) \left\{ e^{-\alpha \tan\varphi} \tan\left(\frac{\pi}{4} - \frac{\varphi}{2}\right) \sin\beta + \cos(\beta - \alpha) \right\}}{\left\{ e^{-\alpha \tan\varphi} \tan\left(\frac{\pi}{4} - \frac{\varphi}{2}\right) \cos\beta - \sin(\beta - \alpha) \right\}}. \end{aligned}\right\} \tag{13}$$

The first failure line $BCDE$ is a line of discontinuity in the velocity field so that the velocity vector along this line must make an angle φ with the line. It follows that $v_2 = 0$ along $BCDE$ and therefore v_2 is zero throughout the plastic region $ABCDE$, since the second failure lines are straight. In the region ADE, v_1 is constant and given by

$$v_1 = v \cos \varphi,$$

where v is the magnitude of the velocity vector in ADE. The boundary condition along AE requires that the velocity of the wedge and that of the soil in contact with it must have the same projection on the normal to AE, and therefore

$$v = \sin \beta \sec \left(\frac{\pi}{4} + \frac{\varphi}{2}\right).$$

In the zone of radial shear the velocity increases exponentially along each first failure line, and along AC the velocity vector has the constant magnitude

$$V = \sin \beta \sec \left(\frac{\pi}{4} + \frac{\varphi}{2}\right) e^{\alpha \tan \varphi}.$$

At a given instant, the region ABC is moving as a rigid body with velocity V in the direction perpendicular to AC. The velocity field in the plastic region is illustrated on the left of Fig. 11.

The projection of the velocity of the lip AB on the normal to AB is

$$V \cos \left(\frac{\pi}{4} - \frac{\varphi}{2}\right) = \sin \beta \tan \left(\frac{\pi}{4} + \frac{\varphi}{2}\right) e^{\alpha \tan \varphi},$$

while the projection of the velocity of the vertex E, which is moving downward with unit velocity, on the normal to AB is $\cos(\beta - \alpha)$. Hence, the distance of E from AB increases at the (constant) rate which is the sum of these two projections. At a time t, i.e., since the beginning of the indentation, the distance of E from AB has therefore reached the value

$$t[\sin \beta \tan \left(\frac{\pi}{4} + \frac{\varphi}{2}\right) e^{\alpha \tan \varphi} + \cos (\beta - \alpha)]. \tag{14}$$

From Fig. 11 we see that this distance is also equal to

$$b + t \cos (\beta - \alpha), \tag{15}$$

and equating the expressions (14) and (15) gives

$$b = t \sin \beta \tan \left(\frac{\pi}{4} + \frac{\varphi}{2}\right) e^{\alpha \tan \varphi}. \tag{16}$$

The substitution of the expressions (13) into this equation furnishes a relation between the angles α, β, and after some reduction we obtain

$$\cos (2\beta - \alpha) = \frac{\cos \alpha \left[e^{\alpha \tan \varphi} \tan \left(\frac{\pi}{4} + \frac{\varphi}{2}\right) + e^{-\alpha \tan \varphi} \tan \left(\frac{\pi}{4} - \frac{\varphi}{2}\right) \right]}{\left\{ 2 \sin \alpha + e^{\alpha \tan \varphi} \tan \left(\frac{\pi}{4} + \frac{\varphi}{2}\right) + e^{-\alpha \tan \varphi} \tan \left(\frac{\pi}{4} - \frac{\varphi}{2}\right) \right\}}. \tag{17}$$

The variation of the angle α with the angle β, obtained from (17), is shown in Fig. 12 for $\varphi = 20°$.

The pressure P on the flank of the wedge can easily be obtained from the pattern of the failure lines and the boundary condition of zero traction along AB. It is found to be given by

$$P = c \cot \varphi \left\{ e^{2\alpha \tan \varphi} \tan^2 \left(\frac{\pi}{4} + \frac{\varphi}{2} \right) - 1 \right\},$$

where, as before, c is the cohesion of the soil.

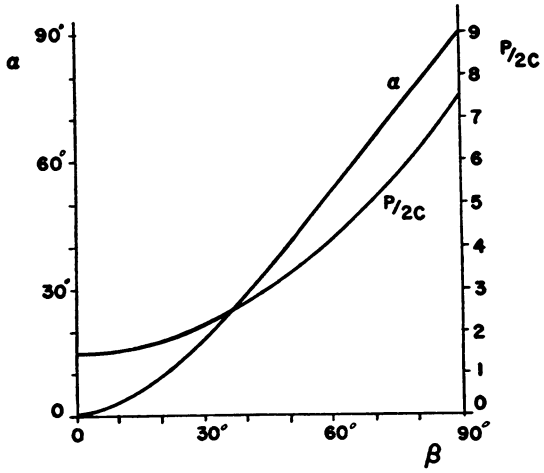

FIG. 12 Variation of P and α with β

The variation of P with the angle β is shown in Fig. 12 for $\varphi = 20°$. Since we have

$$AE = l \tan \left(\frac{\pi}{4} - \frac{\varphi}{2} \right) e^{-\alpha \tan \varphi},$$

the total downward force F necessary to drive the wedge into the soil is given by

$$F = 2Pl \sin \beta \tan \left(\frac{\pi}{4} - \frac{\varphi}{2} \right) e^{-\alpha \tan \varphi}.$$

The determination of the motion of a particular element of the soil appears to be rather complicated since the velocity of the element is influenced by its varying position in space and also by the continual expansion of the velocity field. However, the use of the unit diagram introduced by Hill, Lee and Tupper greatly facilitates the solution. The unit diagram is obtained by transforming the velocity field into a geometrically similar field in which the penetration is always unity. This is effected by the transformation

$$\mathbf{r} = \mathbf{r}^* t,$$

where $\mathbf{r}$ is the actual position vector of the element with reference to O and $\mathbf{r}^*$ is its corresponding position vector in the unit diagram. The method of determining the trajectory of an element is very similar to that used by Hill, Lee and Tupper for the perfectly plastic material and for brevity we omit the details of the solution. The unit diagram,

with three typical trajectories, is given in Fig. 13, and in Fig. 14 we show the deformation of the originally square meshes of a grid, where we have taken $\beta = 30°$, $\varphi = 20°$.

It is also possible to solve the problem when there is a moderate amount of sliding friction between the soil and the wedge. The angle of the wedge must not be too large in order to make it possible to extend the plastic field in a satisfactory manner below the vertex of the wedge. In this case the lines of failure do not meet the flank of the wedge at an angle $\pi/4 + \varphi/2$ but the pressure on the wedge is uniformly distributed. The lip AC is still straight although it is inclined at a smaller angle to the undisturbed surface.

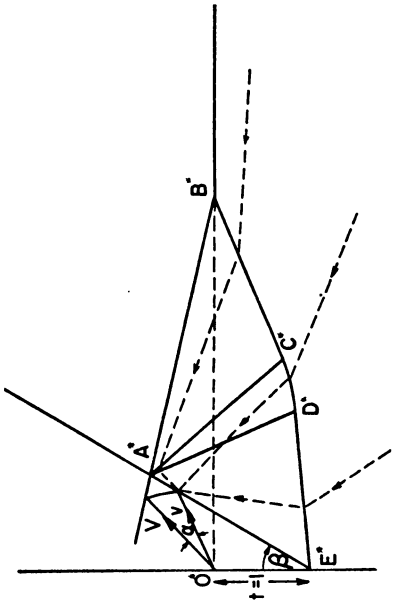

FIG. 13 The Unit Diagram

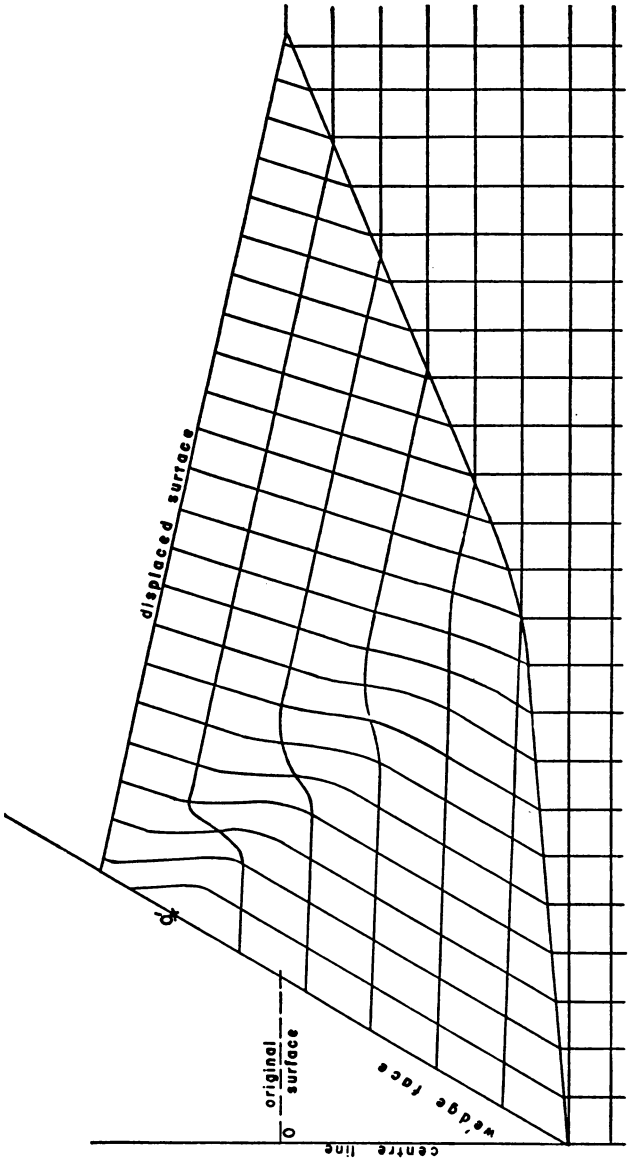

FIG. 14. Deformed grid after indentation by lubricated wedge.

Bibliography

[1] D. C. Drucker and W. Prager, *Soil mechanics and plastic analysis or limit design*, Q. Appl. Math. **10**, (1952).

[2] K. Terzaghi, *Theoretical soil mechanics*, John Wiley and Sons, p. 22, 1943. In this reference, σ_x and and σ_y denote compressive stresses, while in equation (1) σ_x and σ_y are positive when the stresses are tensile.

[3] V. V. Sokolovsky, *Statics of earthy media*, Izdatelstvo Akademii Nauk S. S. R., Moscow, 1942.

[4] F. Kötter, Berlin Akad. Berichte, p. 229, (1903).

[5] R. v. Mises, *Mechanik der plastischen Formaenderung von Kristallen*, Z. angew. Math. Mech. **8**, 161-185 (1928).

[6] L. Prandtl, *Ueber die Haerte plasticher Koerper*, Goettinger Nachr., Math.-Phys. Kl. 1920, 74-85 (1920).

[7] R. Hill, *The plastic yielding of notched bars under tension*, Q. J. Mech. Appl. Math. **2**, 40-52 (1949).

[8] R. Hill, E. H. Lee, and S. J. Tupper, *The theory of wedge indentation of ductile materials*, Proc. Roy. Soc. London (A) **188**, 273-289 (1947).